Desalination and Water Treatment
www.deswater.com

doi:10.5004/dwt.2018.22577

116 (2018) 119–128
June

Comparative evaluation of nitrate adsorption from aqueous solutions using green and red local montmorillonite adsorbents

Rasoul Khosravi[a], Hadi Eslami[b], Ahmad Zarei[c], Mohsen Heidari[d], Abbas Norouzian Baghani[e], Navid Safavi[f], Adel Mokammel[g], Mehdi Fazlzadeh[e,h,*], Shahin Adhami[h]

[a]*Social Determinants of Health Research Center, Department of Environmental Health Engineering, School of Health, Birjand University of Medical Sciences, Birjand, Iran, Tel. +989353281454, email: khosravi.r89@gmail.com (R. Khosravi)*
[b]*Department of Environmental Health Engineering, School of Health, Rafsanjan University of Medical Sciences, Rafsanjan, Iran, email: hadieslami1986@yahoo.com (H. Eslami)*
[c]*Department of Environmental Health Engineering, School of Public Health, Gonabad University of Medical Sciences, Gonabad, Iran, Tel. +985133289748, email: zarei.ahmad@gmail.com (A. Zarei)*
[d]*Department of Environmental Health Engineering, Faculty of Health, Hormozgan University of Medical Sciences, Bandar Abbas, Iran, Tel. +989132615255, email: moheidari84@gmail.com (M. Heidari)*
[e]*Department of Environmental Health Engineering, School of Public Health, Tehran University of Medical Sciences, Tehran, Iran, Tel. +989102141053, email: abbas.jj.norozi@gmail.com (A.N. Baghani)*
[f]*Department of Environmental Health Engineering, School of Health, Tabriz University of Medical Sciences, Tabriz, Iran, Tel. +9841698572, email: Navid.safavi@yahoo.com (N. Safavi)*
[g]*Department of Environmental Health Engineering, School of Health, Ardabil University of Medical Sciences, Ardabil, Iran, Tel. +984533513775, email: adelmokamel@gmail.com (A. Mokammel)*
[h]*Social Determinants of Health Research Center, Ardabil University of Medical Sciences, Ardabil, Iran, Tel. +984515513428, Fax +98 4533512004, email: m.fazlzadeh@gmail.com (M. Fazlzadeh), sh.adhami69@gmail.com (S. Adhami)*

Received 21 June 2017; Accepted 31 May 2018

ABSTRACT

Nitrate has been identified as a major pollutant in water resources. In this study, two new adsorbents, namely, red local montmorillonite (RLM) and green local montmorillonite (GLM)were used as adsorbents, and their characteristics and performance in nitrate adsorption has been investigated. The most important factors in the adsorption process such as initial pH, adsorbent dosage, contact time and initial concentration of nitrate were investigated. Also, EDAX, BET, SEM and FTIR techniques were used to determine adsorbent characteristics. The results showed that the highest nitrate adsorption for both adsorbents obtained at low pH values,and removal efficiency increased by increasing the dosage and contact time and decreased by increasing the initial concentration of nitrate. EDAX technique showed that the amount of MgO in GLM and RLM were 2.6% and 1.4% respectively, indicating a double amount of MgO in GLM structure. MgO can have a very important role in nitrate adsorption but BET technique showed that the specific surface area of RLM is more than GLM. Overall results showed that the adsorption capacities of GLM and RLM were relatively high and the values were 89.2 and 87.7 mg/g, respectively. High adsorption capacity can nominate two new adsorbents for nitrate adsorption. Adsorption process followed the Langmuir isotherm and the experimental data followed the pseudo second-order kinetic. Also, the results of thermodynamic experiments showed that the adsorbing reaction for both adsorbents was exothermic and they occurred spontaneously.

Keywords: Adsorption; Water; Montmorillonite; Nitrate

---

*Corresponding author.

1. Introduction

Water is a key matter in the environment and a cherished gift of the nature to human life, particularly in regions where natural water resources are limited and water shortage is problematic [1,2]. However, water also can be a carrier for various contaminants that can lead to many human health issues [3–5]. In many parts of the world, nitrate is one of the most common pollutants in water resources [6,7]. Nowadays, the problem of high level of nitrates in surface and ground waters has become a controversial issue [8,9]. Sources of nitrates in water resources include the use of agricultural fertilizers, municipal sewerages, animal manures, food industries, detergent industries and also thermal power plants [10–12]. High levels of nitrate in drinking water can cause many problems for human health. Nitrate itself is rather benign, but it can be reduced to toxic nitrite in the human gastrointestinal tract. High concentrations of nitrates can cause blue baby syndrome (methemoglobinemia), especially in children with less than one year old [13–18]. In the body, nitrate converts to nitrite in the stomach and resulting in the formation of nitrosamines which are carcinogenic [19]. High nitrate concentration not only affects human health but also affects the fishes. Nitrate and phosphate causes algae growth and oxygen depletion where it can lead to eutrophication of water bodies which may greatly affects aquatic organisms [20–22]. Because of the unpleasant effects of nitrate on human health, the World Health Organization (WHO) and United States Environmental Protection Agency (US-EPA) has set the maximum allowable concentration of 50 and 45 mg/L in drinking water, respectively [23]. Because of stability and high solubility of nitrate, it can contaminate a large amount of water resources particularly groundwater, and therefore, it is a serious threat to drinking water supplies [24].

Physical-chemical and biological techniques can be used to remove nitrate from water and wastewater. These techniques include adsorption, ion exchange, electrochemical, reverse osmosis, biological de-nitrification, chemical purification, etc. [25–33]. Biological methods require an additional carbon source and also produce large amount of sludge [29,34]. Ion exchange requires disposal system for salty wastes and the high cost of resin regeneration [35]. In the electrochemical process, electrodes can be easily disabled [36,37]. Also, in the reverse osmosis process, operating costs are very high. Among these techniques, adsorption is simpler, more economical and effective, with less sludge production [38] which can be proposed for nitrate removal. However, nowadays the use of this technique is considered by many researchers worldwide [39–42]. In recent years, various adsorbents for nitrate removal from aqueous environment have been tested by many researchers. Among these adsorbents, natural minerals [43,44], activated carbon [45,46], agricultural wastes [47,48] and synthetic minerals [49,50] have reported good results. Thus, it is necessary to remove nitrate economically and efficiently by developing affordable and accessible materials [51]. The aim of this study was to evaluate the efficiency and performance of red and green local montmorillonite obtained from Ardabil's mines, Iran as new adsorbents for the removal of nitrate from aqueous solutions. In this study, the adsorption capacity of the adsorbents and their characteristics are studied by using EDAX, SEM, BET and FTIR techniques.

2. Materials and methods

2.1. Adsorbents preparation

Green and red montmorillonite was obtained from Sarcham region in Ardabil, Iran. Initially, the montmorillonite samples were crushed and screened to obtain uniform particle sizes. After that, the screened sample was sun dried to remove any residual moisture. Then, the soil was washed several times with distillated water to remove dirts and dried at 60ºC for 24 h. Then, the granular particles were separated using a 10 mesh sieve and placed in a dry place for further use [52,53].

2.2. Batch experiments

This experimental study was conducted in a batch manner in 100 mL conical flasks placed on a shaker. Potassium nitrate from Merck was used to prepare desired concentrations of nitrate. After preparation of the adsorbents, 50 mL of the sample with desired concentrations was added into each flask. Solution pH was adjusted using 0.1 N NaOH and HCl. Then, determined amounts of adsorbent is added into each flask, and placed on the shaker with a constant agitation speed. After predetermined time intervals, the samples were removed from the shaker and residual concentrations of nitrate were measured. The effects of various operational parameters such as pH 2,4,6,7,8,11, time of adsorption 1, 5, 10, 15, 20, 30, 60, 75, 90, 120, 150, 180, 210 min, nitrate initial concentration 25, 50, 100, 150, 200, 250 mg/L, and adsorbent dosage 1, 2, 4, 6, 8, 10 g/L on nitrate removal efficiency were investigated. The experiments were repeated in duplicate and the averages were reported.

2.3. Residual nitrate determination and adsorbents characteristics

The residual concentration of nitrate in the solution was measured using a spectrophotometer at wavelength corresponding to the maximum absorbance for the nitrate at 220 nm according to the procedure described in the Standard Methods for the Examination of Water and Wastewater [54]. Brunauer, Emmett and Teller (BET), Fourier Transform Infrared Spectroscopy (FTIR), Scanning Electron Microscope (SEM) and Energy Dispersive X-Ray (EDAX) techniques were used to study the adsorbents characteristics including specific area, and functional groups.

3. Results and discussion

3.1. Adsorbents characteristics

3.1.1. pHzpc determination for red local montmorillonite (RLM) and green local montmorillonite (GLM)

pHzpc for red local montmorillonite (RLM) and green local montmorillonite (GLM) were obtained to be 8.14 and

8.89, respectively, which indicates that at pH values below 8.14 RLM and 8.89 for GLM, the adsorbents have positive charges and at the above this pHs, the adsorbents surfaces is negatively charged. But it is interesting to note that nitrate is an anion with negative charge on its surface.

3.1.2. EDAX technique

Table 1 summarizes chemical analysis of red and green montmorillonite obtained from EDAX technique. In both adsorbents, 90% of components were related to the Fe_2O_3, Cao, Al_2O_3, and SiO_2, but their amounts were different. Higher CaO level in GLM justifies having a higher pHzpc in GLM compared to RLM. Weight percent of other components of the adsorbents were less than 4%. Green montmorillonite has 2.6% MgO, furthermore, RLM contains 1.4% MgO which is twice as that in in the GLM. MgO can drastically bond with anions in aquatic solutions through complexion of the single-core, dual-core and triple-core face [55]. Therefore, existence of MgO in the structure of GLM can increase its ability to adsorb nitrate.

Table 1
Results of EDAX technique to determine the weight percent of the components of RLM and GLM

Wt%	SiO_2	Al_2O_3	CaO	Fe_2O_3	MgO	k_2O	Na_2O	TiO_2
RLM	58.3	17.7	2.8	11	1.4	3.9	1.2	1.4
GLM	56.9	13.5	9.7	9.6	2.6	2.1	1.6	1.3

3.1.3. SEM and BET specific surface area

Fig. 1 shows several micrographs at different magnifications of RLM and GLM. GLM micrograph shows that its surface has more porosity than RLM and also it is rougher. According to Figs. 1a and b, it is evident that the pores on green montmorillonite are deeper, and the presence of pores on its surface provides many sites for the consider-

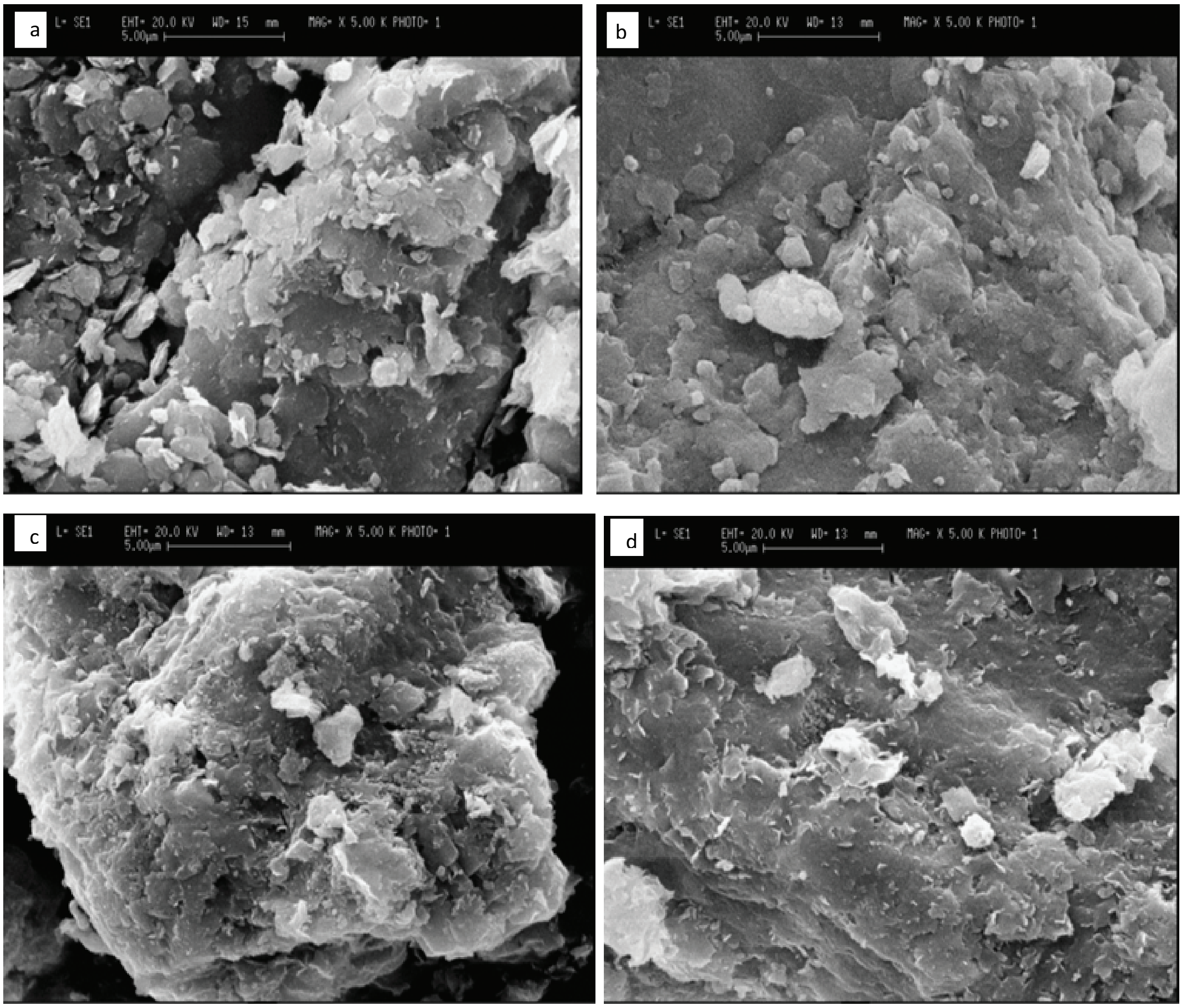

Fig. 1. SEM images of (a) RLM (b) RLM after adsorption (c) GLM and (d) GLM after adsorption.

able penetration and adsorption of the contaminant. BET technique also confirms high volume of pores in GLM compared to RLM. So, the total volume of pores on the GLM and RLM were 0.0739 cm^3/g and 0.0689 cm^3/g, respectively. In addition, BET technique shows that the average of pores diameter on the GLM and RLM are about 23 and 7 nm, respectively. These results can be obviously seen in SEM images taken from the adsorbents surfaces. Existences of more pores with larger diameter provide more suitable and bondable sites for adsorption. But specific surface area of RLM and GLM are 29 m^2/g and 13 m^2/g respectively, which indicate that the specific surface area of RLM is 2.23 times more than GLM. So, it can be stated that although specific surface area is more in RLM compared to GLM, but due to more heterogeneous surface morphology of GLM compared to RLM, green montmorillonite has more active binding sites for nitrate adsorption [56]. Also, SEM micrographs of GLM show that after adsorption, the surface morphology of adsorbent became more homogeneous and its active surfaces also decrease. Despite having less specific surface area in GLM, it has a high adsorption capacity, showing the high tendency of the adsorbent toward nitrate [56].

3.1.4. FTIR study

FTIR test is used to determine the functional groups and their role in nitrate adsorption and its results are illustrated in Figs. 2a and b. In the figure, similar peaks can be seen for both adsorbents, which indicate the adsorbents structure similarity. One of these peaks is the peak between 800 to 1200 cm^{-1} (the highest peaks 1041 and 1081 cm^{-1}), which represents the C-O bonds [56]. There are peaks in the range of 400–850 cm^{-1} (the highest peak 470 and 840 cm^{-1}) that are related to the Al-O and Si-O bonds [13]. The peak between 3600 and 4000 cm^{-1} (the highest peak 3641 cm^{-1}) is related to the O-H bond which is caused by SiO$_2$ groups which is highly efficient for nitrate adsorption [13]. Also peaks between 3200 to 3600 cm^{-1} (the largest peak 3580 cm^{-1}) are related to mutual hydrogenated bonds between O-H and N-H [56].

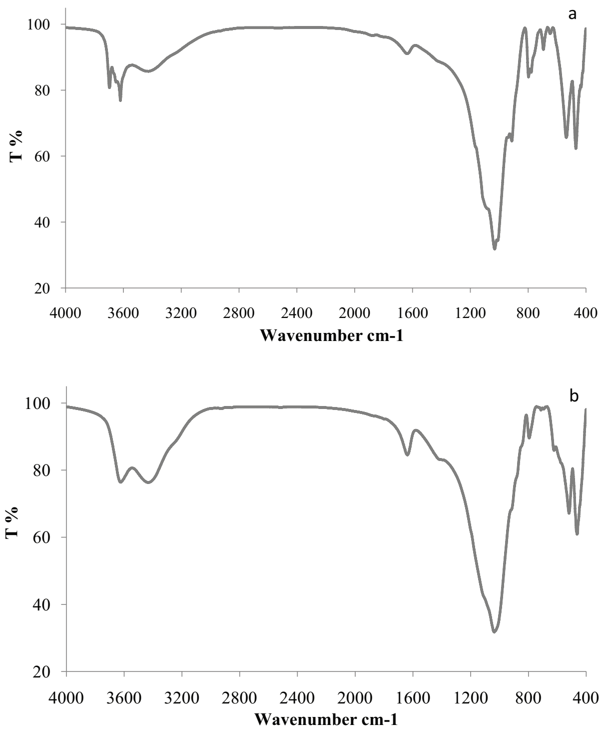

Fig. 2. FTIR spectra of (a) RLM and, (b) GLM.

3.2. Effect of initial pH

pH is one of the influential factors on adsorption process [57,58]. In Fig. 3, results of different pH effects on the efficiency of nitrate removal are investigated for the green and red montmorillonite adsorbents. The results show that by increasing pH from 5.1 to 11, efficiency of nitrate removal is promoted for both adsorbents. By increasing pH from 5.1 to 11, nitrate removal efficiency for red montmorillonite decreased from 80.16 to 58.37%, and for green montmorillonite from 90.18 to 59.38%. Higher pH values increase the number of hydroxide ions, leading to the greater competition between hydroxide and nitrate ions for adsorbing on the adsorbent binding sites, and thus, hydroxide ions increase the penetration resistance of nitrate ions [56,59]. The results of this study is compatible with the results of the other studies such as Öztürk et al. [60], Cengeloglu et al. [59], Ganesan et al. [19] , Hu et al. [56]. Moreover, the point of zero charge (pHzpc) for the adsorbents should be considered. At pH values blow the pHzpc that is 8.14 and 8.89 for RLM and GLM respectively, the surface of adsorbents particles is positively charged and can be suitable for adsorption of anionic materials such as nitrate, and by increasing the pH to above this values, the surface charge of adsorbents changed into negatively that lead to decreasing affinity for anion adsorption.

3.3. Effect of adsorbent dosage

Fig. 4 shows that by increasing adsorbent dosage, removal efficiency increases for both adsorbents. By increasing adsorbent dosage from 1 to 6 g/L, nitrate removal efficiency for red montmorillonite increased from 52.29 to 79.18%, and for green montmorillonite from 70.65 to 91.14%. Adsorbent surface has increased by increasing the amount of adsorbent, therefore the available sites

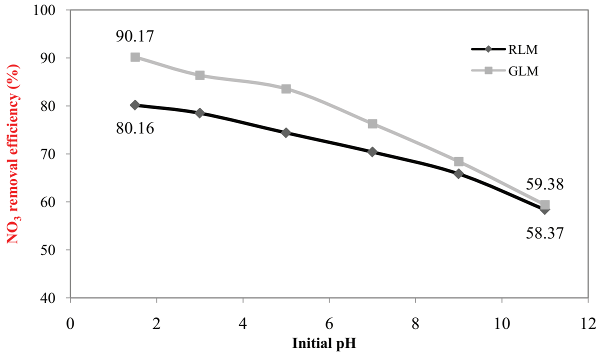

Fig. 3. Effect of initial pH (initial nitrate concentration 25 mg/L, contact time 60 min, adsorbent dosage1 g/L, temperature 23°C and agitation speed 152 rpm).

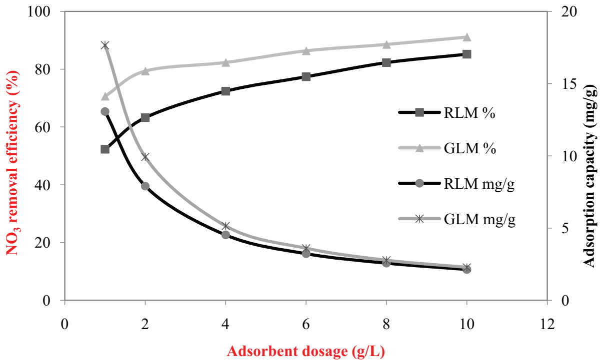

Fig. 4. Effect of adsorbent dosage (initial concentration of nitrate 25 mg/L, contact time of 60 min, initial pH of solution 5.1, temperature 23°C and agitation speed 150 rpm).

for adsorption of pollutants increased, which in general enhanced removal efficiency [60,61]. It can be said that under the same conditions, removal efficiency of green montmorillonite was higher than red montmorillonite, and also the volume of generated sludge increases by increasing adsorbent dosage which is notable from economic and environmental risks perspective. Thus it can be noted that lower amount of GLM can remove more amount of nitrate compared to RLM.

Results also showed that by increasing adsorbent dosage, the adsorption capacity decreases in both adsorbents. In the case of red montmorillonite, with increasing adsorbent dosage from 1 to 6 g/L, adsorption capacity decreased from 13.7 to 2.13 mg/g. As well as in the case of green montmorillonite, with increasing adsorbent dosage from 1 to 6 g/L, adsorption capacity decreased from 17.66 to 2.27 mg/g (Fig. 7). When the dosage of adsorbent is low, all the free binding sites on the adsorbent surfaces are in contact with nitrate, and therefore causes adsorption capacity enhancement. But with increasing the amount of adsorbent, available binding sites with less energy saturate quickly, but nitrate adsorption do not occur in free sites which requires more energy and in this case nitrate adsorption rate increases but its adsorption capacity declines [39,59].This is well-matched with the results of Cengeloglu et al. [59] and Milmile et al. [39].

3.4. Effect of contact time

Fig. 5 shows that by increasing the contact time, the amount of adsorbed nitrate increases for both adsorbents. The amount of adsorbed nitrate by red and green montmorillonite at contact time of 1 min was 4.98 mg/g and 6.81 mg/g, respectively, and by increasing contact time to 150 min, the amount of adsorption for red and green montmorillonite increased to 17.84 mg/g and 20.62 mg/g, respectively. Therefore, the amount of adsorption for green montmorillonite was more than that of red montmorillonite. Increasing contact time tends to create more opportunities for nitrate in the solution to find free sites to adsorb which results in removal efficiency increase [51]. This is similar to the studies such as Öztürk et al. [60] and Cengeloglu et al. [59] which they reported that by increasing contact time, nitrate removal level has increased.

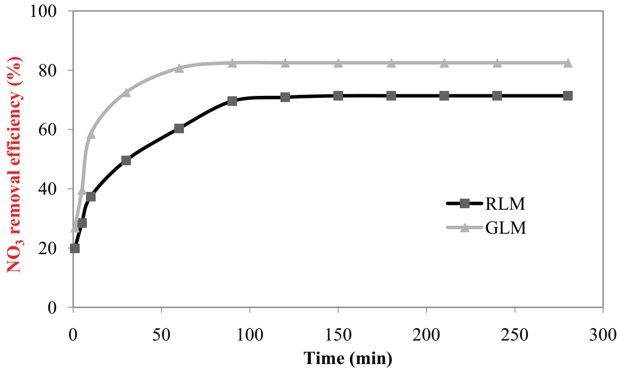

Fig. 5. Effect of contact time (initial concentration of nitrate 25 mg/L, adsorbent dosage 1 g/L, initial pH of solution 7, temperature 23°C and agitation speed 150 rpm).

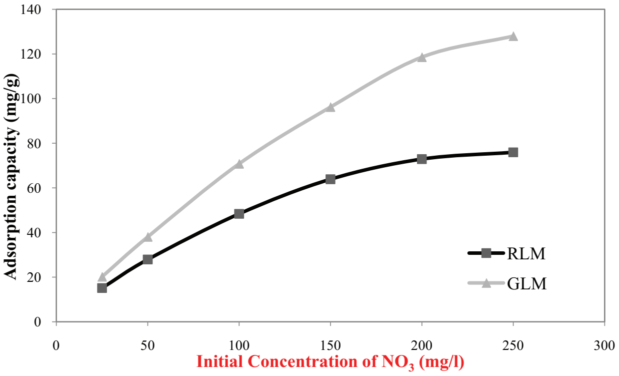

Fig. 6. Effect of initial concentration of nitrate (adsorbent dosage 1 g/L, contact time of 60 min, initial pH of solution 7, temperature 23°C and agitation speed 150 rpm).

3.5. Effect of initial concentration of nitrate

Fig. 6 shows that nitrate adsorption rises by increasing initial concentration of nitrate in both adsorbents. So, at 25 mg/L of initial concentration of nitrate, the amount of nitrate adsorption by red and green montmorillonite was 15.1 mg/g and 20.18 mg/g respectively, and by increasing initial concentration of nitrate to 250 mg/L, the amount of nitrate adsorption by red and green montmorillonite has increased to 75.9 mg/g and 127.9 mg/g, respectively. Increasing nitrate concentration gradient in the solution acts like a driving force to overcome the resistance of mass transfer between the volume of solution and adsorbent surface and consequently increase the adsorption rate [56]. But removal efficiency decreases along with increasing initial concentration of nitrate. Similarly, by increasing initial concentration of nitrate from 25 mg/L to 250 mg/L, nitrate removal efficiency by red and green montmorillonite decreases from 60.38 to 30.37% and from 80.73 to 19.51%, respectively. It can be said that in a certain amount of adsorbent, adsorption sites can adsorb a certain amount of nitrate ions, thus removal efficiency decreases with increasing of nitrate concentration [56], which is compatible with results of the Hu et al. study [56]. Generally, the amount of adsorbed nitrate by green montmorillonite was more than red montmorillonite and this shows that GLM has a higher adsorption capacity for nitrate adsorption.

3.6. Nitrate adsorption isotherm for red and green montmorillonite

In order to express the behavior of nitrate adsorption on the adsorbents, obtained data from isotherm testing phase have been studied on the most common models, including Langmuir and Freundlich [1,62].

The linear form of Langmuir isotherm is as:

$$\text{Langmuir: } \frac{C_e}{q_e} = \frac{1}{K_l \times q_{max}} + \frac{C_e}{q_{max}} \tag{1}$$

where C_e is the final concentration of nitrates mg/L and q_e is the amount of adsorbed nitrate per unit of adsorbent weight mg/g, K_L is Langmuir constant L/mg which expresses the energy of adsorption. K_L and q_{max} are calculated through the intercept and slope of liner plots of C_e/q_e versus C_e [63,64]. Fundamental characteristics of Langmuir isotherm can be expressed by a non-dimensional factor i.e. reversible (separation factor) R_L [65].

$$R_L = \frac{1}{1+\left(q_{max} \times K_L\right)C_0} \tag{2}$$

When R_L become greater than 1, adsorption is unfavorable, and if it is equal to 1, adsorption is linear, and if it is between 0 and 1, adsorption is optimal, and if it is equal to 0, adsorption is irreversible [66].

Freundlich isotherm shows heterogeneous and multilayer adsorption on an adsorbent surface. Linear equation (3) is used for Freundlich isotherm calculation as below:

$$\text{Freundlich: } \ln q_e = \ln K_f + \frac{1}{n}\ln C_e \tag{3}$$

where K_f represents the maximum adsorption capacity (mg/g) and $1/n$ expresses the intensity of adsorption. If n constant is between 1 and 10, it represents desirability of adsorption [67]. K_f and n are determined from the intercept and slope of liner plots of ln q_e versus ln C_e [68].

RLM and GLM isotherms are shown in Fig. 7. Coefficient of linear regression or R^2 at the Langmuir isotherm is higher than Freundlich isotherm in both adsorbents which indicates that the adsorption process obeys Langmuir model for both adsorbents. Therefore, it can be stated that nitrate adsorption process on RLM and GLM is monolayer. Langmuir and Freundlich isotherm parameters are given in Table 2. K_L for GLM is almost more than double of K_L for RLM, which show higher adsorption energy in GLM compared to RLM. In the case of Freundlich isotherm, n constant was between 1 and 10 for both absorbents which indicates an efficient adsorption of the pollutant on both absorbents [13]. Table 3 compares maximum adsorption capacities of nitrate by GLM, RLM and other adsorbents.

3.7. Adsorption kinetics

In this study, pseudo-first and pseudo-second order kinetic models were used to determine constants, equilibrium adsorption capacity and adsorption mechanism at different concentrations on red and green absorbents.

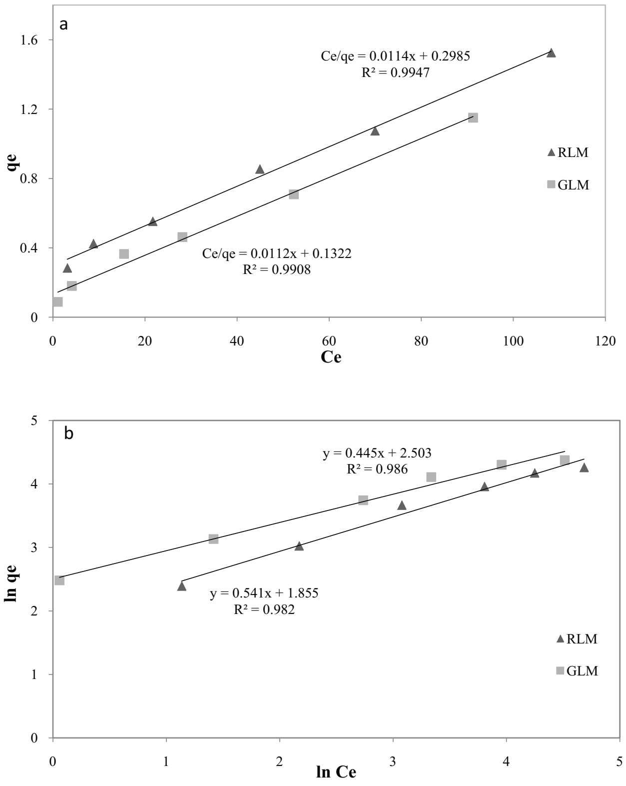

Fig. 7. Adsorption isotherms for nitrate uptake by RLM and GLM adsorbents: Langmuir isotherm (a) and Freundlich isotherm (b).

Table 2
Constants of Langmuir and Freundlich isotherm for GLM and RLM adsorbents

Adsorbent	Langmuir			Freundlich		
	R^2	q_{max}	K_L	R^2	K_F	n
RLM	0.994	87.719	0.038	0.982	6.396	1.847
GLM	0.990	89.286	0.085	0.986	12.219	2.247

Linear form of Lagergren pseudo-first model is as follows [41,69]:

$$\text{Pseudo-first order equation: } \ln\left(q_e - q_t\right) = \ln q_e - K_L t \tag{4}$$

where q_e (mg/g) means nitrate adsorption capacity at equilibrium time, q_t (mg/g) is the amount of nitrate adsorption at t time and K_L (1/min) represents pseudo-first order kinetic constant. K_L and q_e values are calculated from the intercept and slope of linear plots of ln (q_e - q_t) versus t [70,71].

Linear form of Lagergren pseudo-second order model [41,72].

$$\text{Pseudo-second order equation: } \frac{t}{q_t} = \frac{1}{K_2 q_e^{\,2}} + \frac{t}{q_e} \tag{5}$$

Table 3
Comparison of adsorption capacities of nitrate with other adsorbents

Adsorbent	Maximum adsorption capacity (mg/g)	Isotherm model	Ref
Activated bentonite	8.68	Langmuir	[47]
Modified natural clinoptilite	2.5–5.6	–	[48]
modified zeolite	11.4	Freundlich	[49]
Sepiolite	10	Langmuir	[50]
granular chitosan-Fe^{3+}complex	8.35	Langmuir	[39]
Fe–Zr–chitosan	10.6	–	[51]
polyethylene glycol/chitosan	50.68	Freundlich	[52]
polyvinyl alcohol/chitosan	35.03	Freundlich	[52]
modified pine sawdust	22.2-32.8	Langmuir	[40]
RLM	87.7	Langmuir	this study
GLM	89.26	Langmuir	this study

where K_2 (mg/g min) expresses pseudo-second order constant. The values of q_e (slope/1) and K_2 (interception line/slope 2) can calculate through the plots of t/q_t versus t [73].

Laboratory results for both adsorbents follow the pseudo second order model. The values of (R^2) for red and green montmorillonite were equal to 0.990 and 0.999, respectively. The value of K_2 was calculated to obtain the mass transfer rate (Table 4). K_2 values for red and green montmorillonite were 5.8×10^{-3} and 10.7×10^{-3} mg/g min, respectively. According to obtained K_2 values for the adsorbents, it can be stated that nitrate adsorption rate by GLM is about 1.84 times more than nitrate adsorption rate of RLM. Although RLM has more adsorbing surface than GLM, but the results show that the adsorption of the same amount of nitrate by GLM can be done in shorter time than RLM. Therefore, it should be said that functional groups on the surface of GLM compared to RLM have more effective role in nitrate adsorption, and also the presence of superior MgO on the GLM can be the reason of the higher efficiency. Using GLM compared to RLM as an adsorbent can reduce the reaction time, which is very important from economical and operational perspectives.

3.8. Thermodynamics

Temperature is a key factor at the absorption process which can affect adsorption capacity. Results of temperature on nitrate adsorption efficiency are shown in Fig. 9. These results show that by increasing temperature, nitrate removal efficiency in both adsorbents declines. Increasing the number of nitrate ions desorption from the adsorption sites can be one of the possible causes of this behavior [74]. Thermodynamic behavior of nitrate adsorption on RLM and GLM adsorbents calculated by using Gibbs free

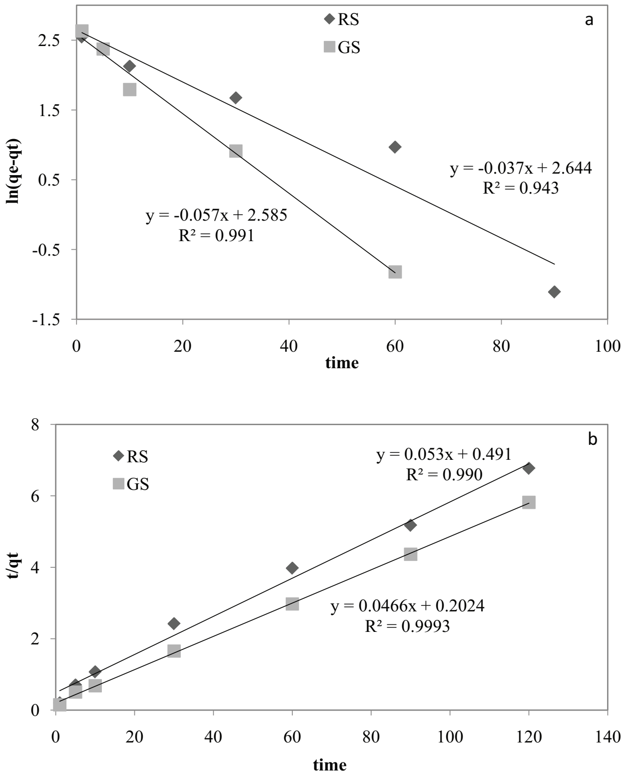

Fig. 8. Pseudo-first order kinetic (a) and pseudo-second order kinetic (b) for RLM and GLM.

Table 4
Constants of nitrate adsorption kinetics on RLM and GLM absorbents

Adsorbent	Pseudo-first order			Pseudo-second order		
	q_e	K_1	R^2	q_e	K_2	R^2
RLM	2.644	–0.037	0.943	18.726	0.0058	0.990
GLM	2.588	–0.057	0.991	21.459	0.0107	0.999

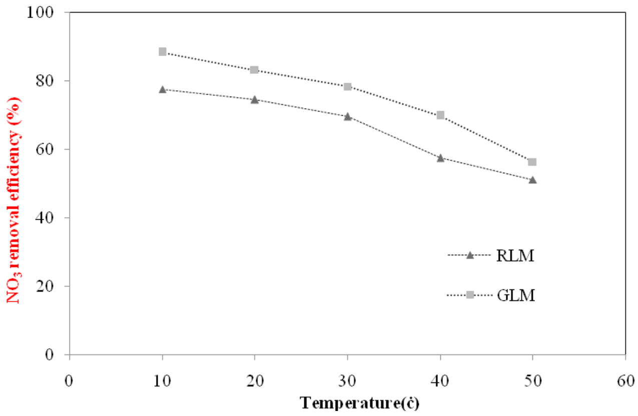

Fig. 9. Effect of temperature on nitrate adsorption (adsorbent dosage 10 g/L, contact time of 60 min, pH of solution 5.1, nitrate concentration of 25 ppm and agitation speed 150 rpm).

energy change (ΔG°), enthalpy changes (ΔH°) and entropy changes (ΔS°) parameters and through following equations [19,75].

$$K_d = \frac{q_e}{C_e} \times \rho \tag{6}$$

$$\Delta G^\circ = -RTLnK_d \tag{7}$$

$$LnK_d = \frac{\Delta S^\circ}{R} - \frac{\Delta H^\circ}{RT} \tag{8}$$

where K_d is the thermodynamic equilibrium constant; ρ is the density of the solution (ρ = 1000 g/L), R and T represent the universal gas constant (8.314 J/mol K) and the system temperature (K), respectively. S° (J/mol·k) and H° (kJ/mol) are determined from the intercept and slope of liner plots of In (K_d) versus 1/T.

Thermodynamic parameters are calculated according to Fig. 10 and Eqs. (6)–(8) and the results are shown in Table 5. The results show that ΔG° is negative for both adsorbents, so it can be stated that nitrate adsorption on RLM and GLM is spontaneous and it is possible in all measured temperature range, and also indicates that these adsorbents have a high tendency toward nitrate adsorption in laboratory conditions [56]. Furthermore, due to the negative ΔH° for both adsorbents, it can be said that nitrate adsorption on RLM and GLM absorbents is exothermic in nature [56].

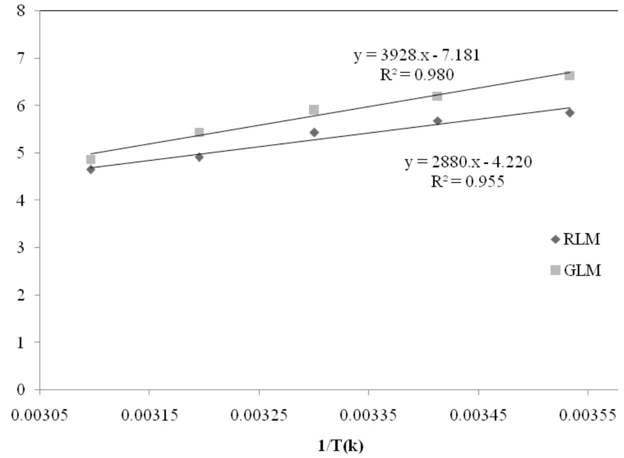

Fig. 10. Van’t Hoff plot for nitrate adsorption by RLM and GLM.

4. Conclusions

In summary, the results demonstrated that GLM and RLM as new adsorbents have high ability to remove nitrate. Specific surface area of RLM is more than GLM, but the results showed that nitrate adsorption rate is more quickly by GLM. GLM due to its different components in comparison to RLM, most notably the presence of more MgO, has higher ability to adsorb nitrate. Adsorption experiments follows by increasing of pH and initial concentration of nitrate, nitrate removal efficiency is decreased for both adsorbents and by increasing adsorbent dosage and contact time, removal efficiency increases for both adsorbents. Laboratory data follows the pseudo second order kinetic and adsorption model has more consistency with Langmuir adsorption model. Thermodynamic tests showed that the nitrate adsorption by RLM and GLM was exothermic and spontaneous in nature.

Acknowledgments

The authors thank Ardabil University of medical sciences because of their financial supports. The authors also thank Professor Mehdi Zarrei at Hospital for Sick Children in Toronto, Canada, for valuable comments and suggestions, allowing us to improve this article.

References

[1] M.H. Dehghani, A. Zarei, A. Mesdaghinia, R. Nabizadeh, M. Alimohammadi, M. Afsharnia, Response surface modeling, isotherm, thermodynamic and optimization study of arsenic (V) removal from aqueous solutions using modified bentonite-chitosan (MBC), Korean J. Chem. Eng., 34 (2017) 757–767.

[2] E. Derakhshani, A. Naghizadeh, A.R. Yari, M.J. Mohammadi, M. Kamranifar, M. Farhang, Association of toxicochemical and microbiological quality of bottled mineral water in Birjand city, Iran, Toxin Rev., 37 (2018) 138–143.

[3] M. Qasemi, M. Afsharnia, A. Zarei, M. Farhang, M. Allahdadi, Non-carcinogenic risk assessment to human health due to intake of fluoride in the groundwater in rural areas of Gonabad and Bajestan, Iran: A case study, Hum. Ecol. Risk Assess., 2018, in press.

[4] M. Ghaderpoori, M. Paydar, A. Zarei, H. Alidadi, A.A. Najafpoor, A.H. Gohary, M. Shams, Health risk assessment of fluoride in water distribution network of Mashhad, Iran, Hum. Ecol. Risk Assess., 2018, in press

[5] M. Masoudinejad, M. Ghaderpoori, A. Zarei, J. Nasehifar, A. Malekzadeh, J. Nasiri, A. Ghaderpoury, Data on phosphorous concentration of rivers feeding into Taham dam in Zanjan, Iran, Data Brief., 17 (2018) 564–569.

[6] A.A. Hekmatzadeh, A. Karimi-Jashni, N. Talebbeydokhti, B. Kløve, Adsorption kinetics of nitrate ions on ion exchange resin, Desalination, 326 (2013) 125–134.

Table 5
Thermodynamic parameters for adsorption of nitrate by two adsorbents

Adsorbent	ΔG° (kJ/mol)					ΔS° (J/mol·k)	ΔH° (kJ/mol)	R^2
	283°k	293°k	303°k	313°k	323°k			
RLM	–13.76	–13.83	–13.69	–12.77	–12.49	–59.70	–32.66	0.955
GLM	–15.62	–15.13	–14.86	–14.17	–13.06	–35.87	–23.94	0.981

[7] M. Pirsaheb, T. Khosravi, M. Fazlzadeh, K. Sharafie, Effects of loading rate, resin height, and bed volume on nitrate removal from drinking water by non-selective strong anion exchange resin (A400E), Desal. Water Treat., 89 (2017) 127–135.

[8] H. Guan, E. Bestland, C. Zhu, H. Zhu, D. Albertsdottir, J. Hutson, C.T. Simmons, M. Ginic-Markovic, X. Tao, A.V. Ellis, Variation in performance of surfactant loading and resulting nitrate removal among four selected natural zeolites, J. Hazard. Mater., 183 (2010) 616–621.

[9] S. Parastar, S. Nasseri, S.H. Borji, M. Fazlzadeh, A.H. Mahvi, A.H. Javadi, M. Gholami, Application of Ag-doped TiO_2 nanoparticle prepared by photodeposition method for nitrate photocatalytic removal from aqueous solutions, Desal. Water Treat., 51 (2013) 7137–7144.

[10] S. Hamoudi, K. Belkacemi, Adsorption of nitrate and phosphate ions from aqueous solutions using organically-functionalized silica materials: Kinetic modeling, Fuel, 110 (2013) 107–113.

[11] P. Loganathan, S. Vigneswaran, J. Kandasamy, Enhanced removal of nitrate from water using surface modification of adsorbents–a review, J. Environ. Manage., 131 (2013) 363–374.

[12] M. Pirsaheb, T. Khosravi, K. Sharafi, M. Mouradi, Comparing operational cost and performance evaluation of electrodialysis and reverse osmosis systems in nitrate removal from drinking water in Golshahr, Mashhad, Desal. Water Treat., 57 (2016) 5391–5397.

[13] C. Mena-Duran, M.S. Kou, T. Lopez, J. Azamar-Barrios, D. Aguilar, M. Dominguez, J. Odriozola, P. Quintana, Nitrate removal using natural clays modified by acid thermoactivation, Appl. Surf. Sci., 253 (2007) 5762–5766.

[14] A. Garron, F. Epron, Use of formic acid as reducing agent for application in catalytic reduction of nitrate in water, Water Res., 39 (2005) 3073–3081.

[15] M.H. Ward, Too much of a good thing? Nitrate from nitrogen fertilizers and cancer, Rev. Environ. Health., 24 (2009) 357–363.

[16] J.A. Camargo, Á. Alonso, Ecological and toxicological effects of inorganic nitrogen pollution in aquatic ecosystems: a global assessment, Environ. Int., 32 (2006) 831–849.

[17] M. Pirsaheb, H. Ghaffari, K. Sharafi, Application of response surface methodology for efficiency analysis of strong non-selective ion exchange resin column (a 400 e) in nitrate removal from groundwater, Int. J. Pharm. Technol., 8 (2016) 11023–11034.

[18] M. Moradi, M. Fazlzadehdavil, M. Pirsaheb, Y. Mansouri, T. Khosravi, K. Sharafi, Response surface methodology (RSM) and its application for optimization of ammonium ions removal from aqueous solutions by pumice as a natural and low cost adsorbent, Arch. Environ. Prot., 42 (2016) 33–43.

[19] P. Ganesan, R. Kamaraj, S. Vasudevan, Application of isotherm, kinetic and thermodynamic models for the adsorption of nitrate ions on graphene from aqueous solution, J. Taiwan Inst. Chem. Eng., 44 (2013) 808–814.

[20] X. Xing, B.-Y. Gao, Q.-Q. Zhong, Q.-Y. Yue, Q. Li, Sorption of nitrate onto amine-crosslinked wheat straw: Characteristics, column sorption and desorption properties, J. Hazard. Mater., 186 (2011) 206–211.

[21] D.J. Conley, H.W. Paerl, R.W. Howarth, D.F. Boesch, S.P. Seitzinger, K.E. Havens, C. Lancelot, G.E. Likens, Controlling eutrophication: nitrogen and phosphorus, Science, 323 (2009) 1014–1015.

[22] Z. Wang, H. Guo, F. Shen, G. Yang, Y. Zhang, Y. Zeng, L. Wang, H. Xiao, S. Deng, Biochar produced from oak sawdust by Lanthanum (La)-involved pyrolysis for adsorption of ammonium (NH_4^+), nitrate (NO_3^-), and phosphate (PO_4^{3-}), Chemosphere, 119 (2015) 646–653.

[23] S. Jain, A. Bansiwal, R.B. Biniwale, S. Milmille, S. Das, S. Tiwari, P.S. Antony, Enhancing adsorption of nitrate using metal impregnated alumina, J. Environ. Chem. Eng., 3 (2015) 2342–2349.

[24] M. Fazlzadeh, K. Rahmani, A. Zarei, H. Abdoallahzadeh, F. Nasiri, R. Khosravi, A novel green synthesis of zero valent iron nanoparticles (NZVI) using three plant extracts and their efficient application for removal of Cr (VI) from aqueous solutions, Adv. Powder Technol., 28 (2017) 122–130.

[25] S. Bagherifam, S. Komarneni, A. Lakzian, A. Fotovat, R. Khorasani, W. Huang, J. Ma, S. Hong, F.S. Cannon, Y. Wang, Highly selective removal of nitrate and perchlorate by organoclay, Appl. Clay Sci., 95 (2014) 126–132.

[26] K. Ota, Y. Amano, M. Aikawa, M. Machida, Removal of nitrate ions from water by activated carbons (ACs)—Influence of surface chemistry of ACs and coexisting chloride and sulfate ions, Appl. Surf. Sci., 276 (2013) 838–842.

[27] S. Kilpimaa, H. Runtti, T. Kangas, U. Lassi, T. Kuokkanen, Removal of phosphate and nitrate over a modified carbon residue from biomass gasification, Chem. Eng. Res. Des., 92 (2014) 1923–1933.

[28] R. Mukherjee, S. De, Adsorptive removal of nitrate from aqueous solution by polyacrylonitrile–alumina nanoparticle mixed matrix hollow-fiber membrane, J. Membr. Sci., 466 (2014) 281–292.

[29] A. Bhatnagar, W. Hogland, M. Marques, M. Sillanpää, An overview of the modification methods of activated carbon for its water treatment applications, Chem. Eng. J., 219 (2013) 499–511.

[30] A. Keränen, T. Leiviskä, B.-Y. Gao, O. Hormi, J. Tanskanen, Preparation of novel anion exchangers from pine sawdust and bark, spruce bark, birch bark and peat for the removal of nitrate, Chem. Eng. Sci., 98 (2013) 59–68.

[31] A. Olgun, N. Atar, S. Wang, Batch and column studies of phosphate and nitrate adsorption on waste solids containing boron impurity, Chem. Eng. J., 222 (2013) 108–119.

[32] J. Chung, K. Amin, S. Kim, S. Yoon, K. Kwon, W. Bae, Autotrophic denitrification of nitrate and nitrite using thiosulfate as an electron donor, Water Res., 58 (2014) 169–178.

[33] M. Alikhani, M. Moghbeli, Ion-exchange polyHIPE type membrane for removing nitrate ions: Preparation, characterization, kinetics and adsorption studies, Chem. Eng. J., 239 (2014) 93–104.

[34] A. Almasi, A. Dargahi, A. Amrane, M. Fazlzadeh, M. Mahmoudi, A. Hashemian, Effect of the retention time and the phenol concentration the stabilization pond efficiency in the treatment of oil refinery wastewater, Fresen. Environ. Bull., 23 (2014) 2541–2548.

[35] C. Shen, Y. Shen, Y. Wen, H. Wang, W. Liu, Fast and highly efficient removal of dyes under alkaline conditions using magnetic chitosan-Fe (III) hydrogel, Water Res., 45 (2011) 5200–5210.

[36] R. Khosravi, M. Fazlzadehdavil, B. Barikbin, H. Hossini, Electro-decolorization of Reactive Red 198 from aqueous solutions using aluminum electrodes systems: modeling and optimization of operating parameters, Desal. Water Treat., 54 (2015) 3152–3160.

[37] R. Khosravi, S. Hazrati, M. Fazlzadeh, Decolorization of AR18 dye solution by electrocoagulation: sludge production and electrode loss in different current densities, Desal. Water Treat., 57 (2016) 14656–14664.

[38] M. Pirsaheb, A. Dargahi, S. Hazrati, M. Fazlzadehdavil, Removal of diazinon and 2, 4-dichlorophenoxyacetic acid (2, 4-D) from aqueous solutions by granular-activated carbon, Desal. Water Treat., 52 (2014) 4350–4355.

[39] S.N. Milmile, J.V. Pande, S. Karmakar, A. Bansiwal, T. Chakrabarti, R.B. Biniwale, Equilibrium isotherm and kinetic modeling of the adsorption of nitrates by anion exchange Indion NSSR resin, Desalination, 276 (2011) 38–44.

[40] G. Nunell, M. Fernandez, P. Bonelli, A. Cukierman, Nitrate uptake improvement by modified activated carbons developed from two species of pine cones, J. Colloid. Interf. Sci., 440 (2015) 102–108.

[41] A. Sowmya, S. Meenakshi, An efficient and regenerable quaternary amine modified chitosan beads for the removal of nitrate and phosphate anions, J. Environ. Chem. Eng., 1 (2013) 906–915.

[42] M. Pirsaheb, Z. Rezai, A. Mansouri, A. Rastegar, A. Alahabadi, A.R. Sani, K. Sharafi, Preparation of the activated carbon from India shrub wood and their application for methylene blue removal: modeling and optimization, Desal. Water Treat., 57 (2016) 5888–5902.

[43] H. Yin, Y. Yun, Y. Zhang, C. Fan, Phosphate removal from wastewaters by a naturally occurring, calcium-rich sepiolite, J. Hazard. Mater., 198 (2011) 362–369.

[44] S. Dikmen, E. Yorukogullari, Nitrate removal from aqueous solution by hexadecyltrimethylammonium bromide-modified clinoptilolite, Asian J. Chem., 23 (2011) 2653.

[45] R. Mahmudov, C.P. Huang, Selective adsorption of oxyanions on activated carbon exemplified by Filtrasorb 400 (F400), Sep. Purif. Technol., 77 (2011) 294–300.

[46] D.-W. Cho, C.-M. Chon, Y. Kim, B.-H. Jeon, F.W. Schwartz, E.-S. Lee, H. Song, Adsorption of nitrate and Cr (VI) by cationic polymer-modified granular activated carbon, Chem. Eng. J., 175 (2011) 298–305.

[47] A.C.A. de Lima, R.F. Nascimento, F.F. de Sousa, M. Josue Filho, A.C. Oliveira, Modified coconut shell fibers: a green and economical sorbent for the removal of anions from aqueous solutions, Chem. Eng. J., 185 (2012) 274–284.

[48] R. Katal, M.S. Baei, H.T. Rahmati, H. Esfandian, Kinetic, isotherm and thermodynamic study of nitrate adsorption from aqueous solution using modified rice husk, J. Ind. Eng. Chem., 18 (2012) 295–302.

[49] M. Islam, R. Patel, Physicochemical characterization and adsorption behavior of Ca/Al chloride hydrotalcite-like compound towards removal of nitrate, J. Hazard. Mater., 190 (2011) 659–668.

[50] M.R. Awual, A. Jyo, T. Ihara, N. Seko, M. Tamada, K.T. Lim, Enhanced trace phosphate removal from water by zirconium (IV) loaded fibrous adsorbent, Water Res., 45 (2011) 4592–4600.

[51] R. Khosravi, M. Fazlzadehdavil, B. Barikbin, A.A. Taghizadeh, Removal of hexavalent chromium from aqueous solution by granular and powdered Peganum Harmala, Appl. Surf. Sci., 292 (2014) 670–677.

[52] M. Fazlzadeh, A. Ahmadfazeli, A. Entezari, A. Shaegi, R. Khosravi, Removal of cephalexin using green montmorillonite loaded with TiO_2 nanoparticles in the presence potassium permanganate from aqueous solution, Koomesh., 18 (2016) 388–396.

[53] R. Khosravi, A. Zarei, M. Heidari, A. Ahmadfazeli, M. Vosughi, M. Fazlzadeh, Application of ZnO and TiO_2 nanoparticles coated onto montmorillonite in the presence of H_2O_2 for efficient removal of cephalexin from aqueous solutions, Korean J. Chem. Eng., 35 (2018) 1000–1008 .

[54] American Public Health Association (APHA). 2017. American Water Works Association (AWWA), Water Environment Federation, 23rd Edition. Washington DC, USA.

[55] M. Zhang, B. Gao, Y. Yao, Y. Xue, M. Inyang, Synthesis of porous MgO-biochar nanocomposites for removal of phosphate and nitrate from aqueous solutions, Chem. Eng. J., 210 (2012) 26–32.

[56] Q. Hu, N. Chen, C. Feng, W. Hu, Nitrate adsorption from aqueous solution using granular chitosan-Fe^{3+} complex, Appl. Surf. Sci., 347 (2015) 1–9.

[57] A.A. Najafpoor, A. Sadeghi, H. Alidadi, M. Davoudi, B. Mohebrad, A. Hosseinzadeh, S. Jafarpour, A. Zarei, Biodegradation of high concentrations of phenol by Baker's Yeast in anaerobic sequencing batch reactor, Environ. Health Eng. Manag. J., 2 (2015) 79–86.

[58] M.H. Dehghani, Z.S. Niasar, M.R. Mehrnia, M. Shayeghi, M.A. Al-Ghouti, B. Heibati, G. McKay, K. Yetilmezsoy, Optimizing the removal of organophosphorus pesticide malathion from water using multi-walled carbon nanotubes, Chem. Eng. J., 310 (2017) 22–32.

[59] Y. Cengeloglu, A. Tor, M. Ersoz, G. Arslan, Removal of nitrate from aqueous solution by using red mud, Sep. Purif. Technol., 51 (2006) 374–378.

[60] N. Öztürk, T.E. Bektaş, Nitrate removal from aqueous solution by adsorption onto various materials, J. Hazard. Mater., 112 (2004) 155–162.

[61] R.A. Rao, F. Rehman, Adsorption studies on fruits of Gular (Ficus glomerata): Removal of Cr (VI) from synthetic wastewater, J. Hazard. Mater., 181 (2010) 405–412.

[62] M.H. Dehghani, A. Zarei, A. Mesdaghinia, R. Nabizadeh, M. Alimohammadi, M. Afsharnia, Adsorption of Cr (VI) ions from aqueous systems using thermally sodium organo-bentonite biopolymer composite (TSOBC): response surface methodology, isotherm, kinetic and thermodynamic studies, Desal. Water Treat., 85 (2017) 298–312.

[63] M. Qasemi, M. Afsharnia, A. Zarei, A.A. Najafpoor, S. Salari, M. Shams, Phenol removal from aqueous solution using Citrullus colocynthis waste ash, Data Brief., 18 (2018) 620–628.

[64] M.H. Dehghani, M. Farhang, M. Alimohammadi, M. Afsharnia, G. Mckay, Adsorptive removal of fluoride from water by activated carbon derived from $CaCl_2$-modified Crocus sativus leaves: Equilibrium adsorption isotherms, optimization, and influence of anions, Chem. Eng. Commun., 205 (2018) 955–965.

[65] S. Chatterjee, S.H. Woo, The removal of nitrate from aqueous solutions by chitosan hydrogel beads, J. Hazard. Mater., 164 (2009) 1012–1018.

[66] S. Norouzi, M. Heidari, V. Alipour, O. Rahmanian, M. Fazlzadeh, F. Mohammadi-Moghadam, H. Nourmoradi, B. Goudarzi, K. Dindarloo, Preparation, characterization and Cr (VI) adsorption evaluation of NaOH-activated carbon produced from Date Press Cake; an agro-industrial waste, Bioresource Technol., 258 (2018) 48–56.

[67] M. Fazlzadeh, R. Khosravi, A. Zarei, Green synthesis of zinc oxide nanoparticles using Peganum harmala seed extract, and loaded on Peganum harmala seed powdered activated carbon as new adsorbent for removal of Cr (VI) from aqueous solution, Ecol. Eng., 103 (2017) 180–190.

[68] M.S. Bilgili, Adsorption of 4-chlorophenol from aqueous solutions by xad-4 resin: isotherm, kinetic, and thermodynamic analysis, J. Hazard. Mater., 137 (2006) 157–164.

[69] A. Naghizadeh, H. Shahabi, F. Ghasemi, A. Zarei, Synthesis of walnut shell modified with titanium dioxide and zinc oxide nanoparticles for efficient removal of humic acid from aqueous solutions, J. Water Health., 14 (2016) 989–997.

[70] A. Mohsenibandpei, A. Alinejad, H. Bahrami, M. Ghaderpoori, Water solution polishing of nitrate using potassium permanganate modified zeolite: parametric experiments, kinetics and equilibrium analysis, Global Nest J., 18 (2016) 546–558.

[71] S. Golmohammadi, M. Ahmadpour, A. Mohammadi, A. Alinejad, N. Mirzaei, M. Ghaderpoori, A. Ghaderpoori, Removal of blue cat 41 dye from aqueous solutions with ZnO nanoparticles in combination with US and US-H_2O_2 advanced oxidation processes, Environ. Eng. Manag. J., 3 (2016) 107–113.

[72] M. Shams, M.H. Dehghani, R. Nabizadeh, A. Mesdaghinia, M. Alimohammadi, A.A. Najafpoor, Adsorption of phosphorus from aqueous solution by cubic zeolitic imidazolate framework-8: Modeling, mechanical agitation versus sonication, J. Mol. Liq., 224 (2016) 151–157.

[73] S. Agarwal, I. Tyagi, V.K. Gupta, M. Dehghani, J. Jaafari, D. Balarak, M. Asif, Rapid removal of noxious nickel (II) using novel γ-alumina nanoparticles and multiwalled carbon nanotubes: Kinetic and isotherm studies, J. Mol. Liq., 224 (2016) 618–623.

[74] G.F. Wasse Bekele, N. Fernandez, Removal of nitrate ion from aqueous solution by modified Ethiopian bentonite clay, Int. J. Res. Pharm. Chem., 4 (2014) 192–201.

[75] H. Biglari, A. Zarei, Direct Blue 71 removal from aqueous solutions by adsorption on pistachio hull waste: equilibrium, kinetic and thermodynamic studies, Iranian J. Health Sci., 4 (2016) 55–70.